JACS
JOURNAL OF THE AMERICAN CHEMICAL SOCIETY
Communication
pubs.acs.org/JACS

A Metal Organic Framework with Spherical Protein Nodes: Rational Chemical Design of 3D Protein Crystals

Pamela A. Sontz,[‡] Jake B. Bailey,[‡] Sunhyung Ahn, and F. Akif Tezcan*

Department of Chemistry and Biochemistry, University of California, San Diego, 9500 Gilman Drive, La Jolla, California 92093, United States

Supporting Information

ABSTRACT: We describe here the construction of a three-dimensional, porous, crystalline framework formed by spherical protein nodes that assemble into a prescribed lattice arrangement through metal−organic linker-directed interactions. The octahedral iron storage enzyme, ferritin, was engineered in its C_3 symmetric pores with tripodal Zn coordination sites. Dynamic light scattering and crystallographic studies established that this Zn-ferritin construct could robustly self-assemble into the desired bcc-type crystals upon coordination of a ditopic linker bearing hydroxamic acid functional groups. This system represents the first example of a ternary protein−metal−organic crystalline framework whose formation is fully dependent on each of its three components.

Design of crystalline materials with tunable structural, chemical, and physical properties represents a major goal common to numerous scientific disciplines.[1−4] Proteins are especially attractive building blocks for crystalline materials as they provide high chemical and structural diversity and possess inherent functions such as catalysis, electron transfer, and molecular recognition. Three-dimensional (3D) protein lattices have been proposed as stable, porous scaffolds for carrying out catalytic reactions under harsh, nonbiological conditions.[5,6] Importantly, the formation of ordered, 3D protein crystals is the foundation as well as the rate-limiting step of protein crystallography, providing a strong motivation for their rational design. Yet, historically, the process of protein crystallization has been largely carried out in a trial-and-error fashion. Although effective methodologies have been developed for facilitating protein crystallization,[7,8] successes in obtaining 3D protein crystals by design have been rare.[9−11] In contrast, the ability to rationally engineer crystalline materials from small organic and inorganic building blocks, though still challenging, is considerably more advanced.[1,12−14] A prominent class of these crystalline materials is metal−organic frameworks (MOFs), which have attracted much attention due their applications in separation, storage, and catalysis, etc.[12,15−23] The wide-ranging applications of MOFs are largely fueled by their modular construction from metal centers (nodes) and organic linkers (struts), which can be used in an interchangeable fashion to create a vast library of structures.[24,25] Following the construction principles of MOFs, we demonstrate here the rational design of a porous 3D protein crystalline framework assembled through metal- and organic linker-directed interactions.

In MOFs, the lattice structure is dictated by the combination of the inherent symmetries of both the metal nodes and the organic struts.[24,25] We envisioned a system where the metal node is a symmetrical protein that displays stable, surface-anchored metal ions. This hybrid protein−metal unit could then self-assemble into the desired 3D lattices via the coordination of symmetric polytopic organic linkers. As an appropriate protein scaffold, we selected the highly stable human heavy-chain ferritin, which is a spherical, cage-like protein with octahedral (432) symmetry (Figure 1).[26,27]

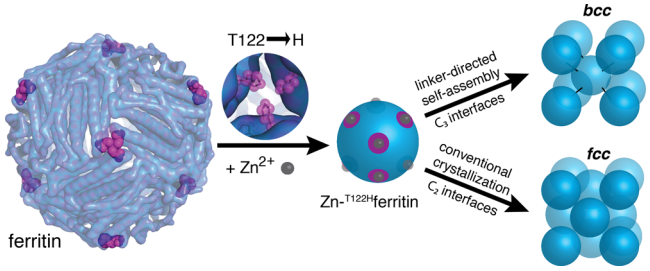

Figure 1. Scheme for metal/linker-directed self-assembly of ferritin into 3D crystals. Surface-exposed binding sites for Zn^{2+} (gray spheres) are engineered at the C_3 pores (magenta) through the T122H mutation. In the presence of ditopic organic linkers, the resulting ^{T122H}ferritin variant is expected to form a bcc lattice.

This symmetry, resembling that of the metal nodes in some quintessential MOFs (e.g., MOF-5,[28] HKUST-1,[16] MIL-53[29]), provides several surface sites lying at or near the C_4, C_3, and C_2 rotation axes which could potentially be engineered for anchoring metal ions. Upon inspection, we deemed the amino acid position 122 (originally threonine) lining the C_3 symmetric pores near the exterior surface (Figure 1) to be well-suited for constructing a tripodal coordination motif for a metal ion with tetrahedral geometry (e.g., Zn^{2+}). The side chains at these positions are oriented toward the center of the pores with α-C distances of 10.2 Å, which provides sufficient clearance for substitution with histidine residues (^{T122H}ferritin) to enable metal coordination.

To probe the formation of the metal−protein node with the desired coordination motifs, ^{T122H}ferritin (12.5 μM) was

Received: July 17, 2015
Published: August 25, 2015

DOI: 10.1021/jacs.5b07463
J. Am. Chem. Soc. 2015, 137, 11598−11601

crystallized by vapor diffusion in the presence of excess $ZnCl_2$ (0.5 mM; to saturate all potential Zn binding sites within the ferritin cage) at pH 8.5. This particular ferritin variant contains the following mutations which eliminate all cysteine residues: C90E, C102A, C130A.[30] Also included was the mutation K86Q, which was shown in a previous study by Lawson et al. to promote the crystallization of ferritin in a face-centered cubic (fcc) lattice through direct metal-mediated crystal packing interactions.[31] These conditions yielded crystals with a characteristic octahedral morphology (Figure 2a) and allowed

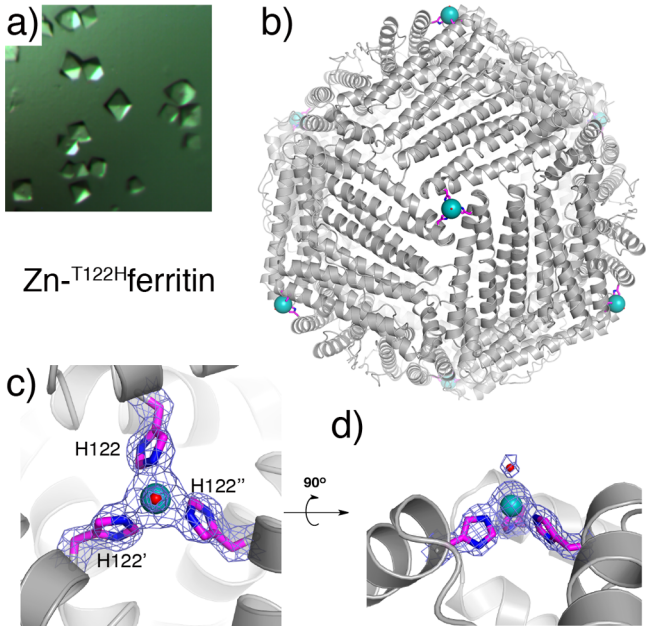

Figure 2. (a) Light micrograph of octahedral fcc crystals of Zn-^{T122H}ferritin. (b) Crystal structure of Zn-^{T122H}ferritin, highlighting the locations of engineered Zn (teal) coordination sites (magenta) in the C_3 pores. (c,d) Closeup views of the engineered Zn coordination sites (water: red sphere). The $2F_o-F_c$ map is contoured at 1σ.

the determination of the Zn-^{T122H}ferritin structure at 1.93 Å resolution (*F*432 space group, $a = b = c = 180.21$ Å; Table S1). This structure shows that the engineered His122 coordination sites in the C_3 pores are occupied with Zn^{2+} ions (8 ions per 24mer, Figure 2b). Importantly, in the fcc arrangement, the His122-Zn sites are far removed from crystal packing contacts formed near the C_2 symmetry axes of ferritin (Figure S1). The engineered Zn coordination sites in the C_3 pores possess a near-ideal tetrahedral geometry formed by the ε-N's of the three His122 side chains and a single water molecule (Figure 2c). The N(His)−Zn−N(His) and N(His)−Zn−OH_2 angles are 109.6° and 109.4°, with Zn−N(His) and Zn−OH_2 bond distances of 2.2 and 2.8 Å, respectively. The distances between the α-C's at position 122 have increased from 10.2 to 10.7 Å, indicating that the C_3 pore has slightly expanded to accommodate stable Zn^{2+} coordination. Importantly, the Zn-bound water molecule protrudes out of the exterior ferritin surface, indicating that it is poised for substitution by the metal-binding moiety of an organic linker.

Given the large size of Zn-^{T122H}ferritin nodes (12 nm diameter) relative to organic linkers used in MOFs, an appropriate linker-mediated supramolecular arrangement would be one directed by a ditopic linker to yield a body-centered cubic (bcc) lattice (Figure 1). We first examined the linker-mediated self-assembly of Zn-^{T122H}ferritin in solution using dynamic light scattering (DLS). DLS measurements with ^{T122H}ferritin (33 μM monomer, 1.4 μM 24-mer) in the presence of excess Zn (75 μM) showed a monodisperse distribution of hydrodynamic diameters (D_h) centered at 13 nm, indicating Zn^{2+} alone does not mediate protein self-assembly (Figure 3a).

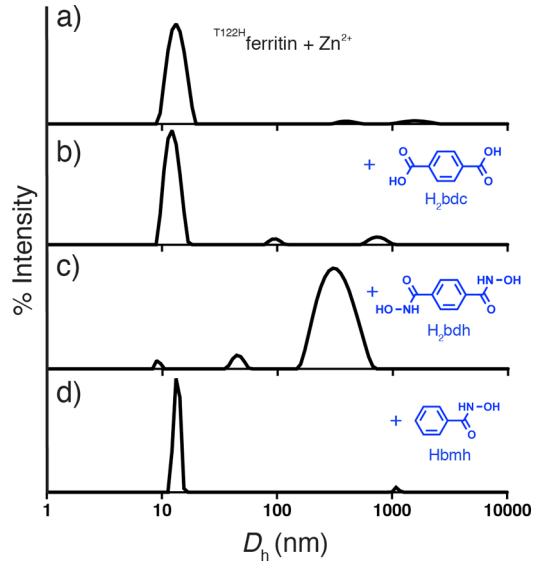

Figure 3. DLS profiles for ^{T122H}ferritin (1.4 μM) in the presence of (a) Zn^{2+} (75 μM), (b) Zn^{2+} (75 μM) + H_2bdc (1 mM), (c) Zn^{2+} (75 μM) + H_2bdh (1 mM), and (d) Zn^{2+} (75 μM) + Hbmh (1 mM). All samples were prepared in a solution containing 50 mM CHES (pH 8.5) and 150 mM NaCl.

The oft-used benzene-1,4-dicarboxylic acid (H_2bdc)[28,29,32] was chosen as the initial candidate for a linker since it is rigid, linear, and water-soluble. We observed that the addition of excess H_2bdc (up to 1 mM) also did not result in significant changes in particle size distribution (Figure 3b). This observation is perhaps not surprising, as the carboxylate functionalities of H_2bdc likely do not provide a sufficiently high affinity for Zn^{2+} to hold together Zn-^{T122H}ferritin nodes in an aqueous medium. We surmised that the substitution of carboxylates with bidentate hydroxamate moieties (frequently used as inhibitors of Zn metalloenzymes)[33−36] could provide the necessary Zn^{2+} binding affinity while preserving the aforementioned properties of H_2bdc. Indeed, the addition of benzene-1,4-dihydroxamic acid (H_2bdh) to a solution of ^{T122H}ferritin and Zn^{2+} led to the complete depletion of the 13 nm diameter species and the emergence of larger aggregates (>300 nm) (Figure 3c). When benzenehydroxamic acid (Hbmh), which cannot act as a linker, was used instead (Figure 3d), or when Zn^{2+} was omitted (Figure S2), no high-order species were observed. These findings indicate that H_2bdh is capable of inducing the self-assembly of Zn-^{T122H}ferritin.

In order to obtain 3D Zn-^{T122H}ferritin crystals through bdh-mediated interactions, we screened a wide range of solution conditions (pH 5.5−9.5) at room temperature. We consistently observed the formation of distinct, rhombic dodecahedral crystals at pH 8.0−9.0 under the following component concentrations: 1−12.5 μM ^{T122H}ferritin or $^{Q86A/T122H}$ferritin (where the Q86A mutation is intended to eliminate the possibility of fcc packing), 50−250 equiv of Zn^{2+} (per 24-meric ferritin unit; to saturate all possible Zn sites), 0.5−2 mM

DOI: 10.1021/jacs.5b07463
J. Am. Chem. Soc. 2015, 137, 11598−11601

H_2bdh. Crystal formation from bulk solution occurred rapidly (<24 h) to form crystals up to 0.5 mm in size (Figure 4a).

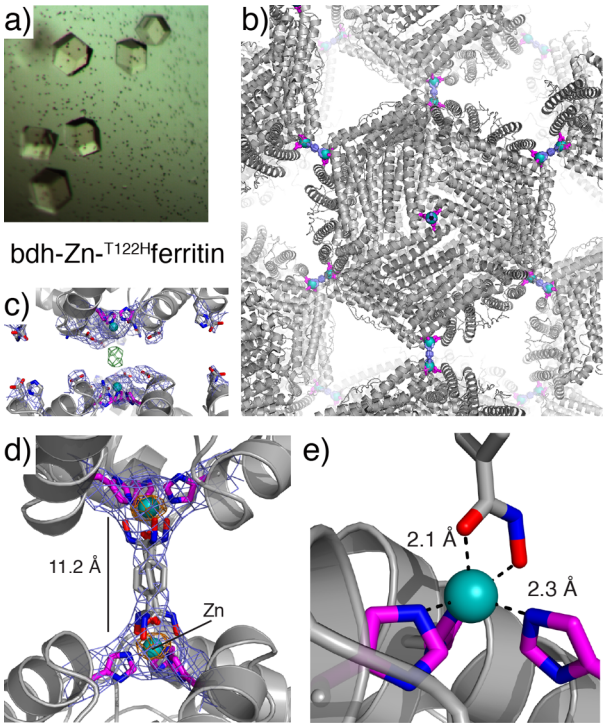

Figure 4. (a) Light micrograph of rhombic dodecahedral bcc crystals of bdh-Zn-^{T122H}ferritin. (b) The bcc packing of the bdh-Zn-^{T122H}ferritin lattice, mediated by bdh^{2-} bridges across the C_3 symmetric ferritin interfaces. (c) View of C_3 symmetric interfaces between neighboring ferritin molecules, showing the lack of direct protein−protein contacts and the presence of electron density between engineered Zn^{2+} ions ($2F_o-F_c$ map: blue-1σ; F_o-F_c map: green-3σ). (d) Closeup view of the three crystallographically related bdh^{2-} rotamers that bridge neighboring ferritin cages; anomalous difference map (7σ) calculated using Zn K-edge diffraction data is shown in orange. (e) Modeled bdh-Zn coordination.

Consistent with DLS measurements, no crystals formed when H_2bdh was substituted with H_2bdc or Hbmh or when any one of the three components (protein, metal, or linker) was not included in solution. When the missing component was introduced into the two-component solutions, which had been incubating overnight, rhombic dodecahedral crystals rapidly emerged. Thus, the self-assembly of bdh-Zn-^{T122H}ferritin crystals is robust and dependent on all three components in solution.

Most of the bdh-Zn-^{T122H}ferritin crystals displayed X-ray diffraction >6 Å, but after an exhaustive screen, we found a crystal that provided sufficiently high resolution (3.79 Å) for structure determination (Table S1) (Figure 4). As designed, this crystal has a bcc lattice arrangement ($I432$ space group, $a = b = c = 155.3$ Å). An inspection of the initial molecular replacement solution reveals a striking picture where ferritin molecules appear to be suspended in the lattice without any protein−protein contacts (Figure S3): the shortest atom-to-atom distance between the neighboring Zn-^{T122H}ferritin nodes near their C_3 symmetry axes is >6 Å (Figure 4c). The engineered Zn^{2+} ions, which lie on the crystallographic C_3 axes, are at a separation of 11.2 Å across the interface with some electron density in the intervening region, consistent with the presence of a linker molecule (Figures 4c). Accordingly, we were able to model a bdh^{2-} linker between the Zn^{2+} ions, where the linker is centered at the intersection of the crystallographic C_2 and C_3 symmetry axes and slightly tilted with respect to the latter (Figure 4d). Because the bdh^{2-} linker lacks three-fold rotational symmetry, it cannot occupy a unique orientation with respect to the two His122-Zn coordination sites that it bridges. The ensuing rotational averaging of bdh^{2-} about the crystallographic C_3 axis, coupled with the low resolution of the diffraction data, gives rise to weak electron density for the linker, particularly around hydroxylamine moieties that are tilted furthest away from the C_3 axis. Nevertheless, a plausible bidentate Zn-bdh coordination geometry can be modeled. In this coordination geometry (shared by three crystallographically related rotamers, Figure 4d), hydroxamate-Zn coordination yields planar five-membered rings with Zn−O(carbonyl) and Zn−O(hydroxylamine) distances of ∼2.1 and 2.3 Å, respectively. The Zn−O(carbonyl) bond is directed nearly parallel to the crystallographic C_3 axis, whereas the Zn−O(hydroxylamine) bond points away from it (at a ∼60° tilt) and between the His122 side chains.

Although other supramolecular protein architectures have been assembled through the use of synthetic organic groups with metal coordinating functionalities[37−42] or pre-existing MOFs have been postsynthetically modified with proteins,[43] the bdh-Zn-^{T122H}ferritin system represents the first example of a ternary protein−metal−organic crystalline framework where each component is an integral part of the construction. The bcc arrangement presents a relatively high packing density for a spherical building block (packing factor = 0.68), yet the ferritin hubs themselves are hollow, thus producing a highly porous framework with a solvent content of 67%. As a result, bdh-Zn-^{T122H}ferritin crystals are highly permeable to solutes, allowing the ferritin hubs to perform their native enzymatic activity within the lattice, which is the oxidation of soluble Fe^{2+} into crystalline Fe^{3+}-oxide mineral (Figure S4). This in crystallo enzymatic activity creates the future opportunity to template crystalline inorganic materials in 3D with nanoscopic precision, particularly if the stability of the frameworks can be improved. More generally, the bdh-Zn-^{T122H}ferritin crystals introduce a new class of hybrid materials that combine the chemical and structural versatility of metal ions, organic linkers, and protein building blocks in a modular fashion.

■ ASSOCIATED CONTENT

Supporting Information

The Supporting Information is available free of charge on the ACS Publications website at DOI: 10.1021/jacs.5b07463.

Materials and methods, Figures S1−S4, and Table S1 (PDF)
(CIF)
(CIF)
(CIF)
(CIF)

■ AUTHOR INFORMATION

Corresponding Author

*tezcan@ucsd.edu

Author Contributions

‡These authors contributed equally.

Notes

The authors declare no competing financial interest.

DOI: 10.1021/jacs.5b07463
J. Am. Chem. Soc. 2015, 137, 11598−11601

■ ACKNOWLEDGMENTS

We thank C. Moore, A. Rheingold, M. Denny, H. Fei, D. Puerta, and S. Cohen for helpful discussions. This work was supported by the US Department of Energy (DOE) (Division of Materials Sciences, Office of Basic Energy Sciences, Award DE-FG02-10ER46677 to F.A.T.). Crystallographic data were collected at SSRL, supported by the DOE, Offices of Basic Energy Sciences and Biological and Environmental Research as well as by the NIH. Coordinate and structure factor files were deposited into the Protein Data Bank under accession numbers 5CMQ and 5CMR.

■ REFERENCES

(1) Moulton, B.; Zaworotko, M. J. *Chem. Rev.* **2001**, *101*, 1629.
(2) Desiraju, G. R. *Angew. Chem., Int. Ed.* **2007**, *46*, 8342.
(3) Hollingsworth, M. D. *Science* **2002**, *296*, 2410.
(4) Dandekar, P.; Kuvadia, Z. B.; Doherty, M. F. *Annu. Rev. Mater. Res.* **2013**, *43*, 359.
(5) Margolin, A. L.; Navia, M. A. *Angew. Chem., Int. Ed.* **2001**, *40*, 2204.
(6) Ueno, T. *Chem. - Eur. J.* **2013**, *19*, 9096.
(7) Cooper, D. R.; Boczek, T.; Grelewska, K.; Pinkowska, M.; Sikorska, M.; Zawadzki, M.; Derewenda, Z.; Acta Crystallogr. *Acta Crystallogr., Sect. D: Biol. Crystallogr.* **2007**, *63*, 636.
(8) Derewenda, Z. S. *Acta Crystallogr., Sect. D: Biol. Crystallogr.* **2010**, *66*, 604.
(9) Lanci, C. J.; MacDermaid, C. M.; Kang, S. G.; Acharya, R.; North, B.; Yang, X.; Qiu, X. J.; DeGrado, W. F.; Saven, J. G. *Proc. Natl. Acad. Sci. U. S. A.* **2012**, *109*, 7304.
(10) Sakai, F.; Yang, G.; Weiss, M. S.; Liu, Y.; Chen, G.; Jiang, M. *Nat. Commun.* **2014**, *5*, 4634.
(11) Brodin, J. D.; Ambroggio, X. I.; Tang, C.; Parent, K. N.; Baker, T. S.; Tezcan, F. A. *Nat. Chem.* **2012**, *4*, 375.
(12) Furukawa, H.; Cordova, K. E.; O'Keeffe, M.; Yaghi, O. M. *Science* **2013**, *341*, 1230444.
(13) Jones, J. T. A.; Hasell, T.; Wu, X.; Bacsa, J.; Jelfs, K. E.; Schmidtmann, M.; Chong, S. Y.; Adams, D. J.; Trewin, A.; Schiffman, F.; Cora, F.; Slater, B.; Steiner, A.; Day, G. M.; Cooper, A. I. *Nature* **2011**, *474*, 367.
(14) Farha, O. K.; Özgür Yazaydın, A.; Eryazici, I.; Malliakas, C. D.; Hauser, B. G.; Kanatzidis, M. G.; Nguyen, S. T.; Snurr, R. Q.; Hupp, J. T. *Nat. Chem.* **2010**, *2*, 944.
(15) Peplow, M. *Nature* **2015**, *520*, 148.
(16) Chui, S. S.-Y.; Lo, S. M.-F.; Charmant, J. P. H.; Orpen, A. G.; Williams, I. D. *Science* **1999**, *283*, 1148.
(17) Li, J. R.; Sculley, J.; Zhou, H. C. *Chem. Rev.* **2012**, *112*, 869.
(18) Liu, J.; Chen, L.; Cui, H.; Zhang, J.; Zhang, L.; Su, C. Y. *Chem. Soc. Rev.* **2014**, *43*, 6011.
(19) Horike, S.; Shimomura, S.; Kitagawa, S. *Nat. Chem.* **2009**, *1*, 695.
(20) Yoon, M.; Srirambalaji, R.; Kim, K. *Chem. Rev.* **2012**, *112*, 1196.
(21) Sumida, K.; Rogow, D. L.; Mason, J. A.; McDonald, T. M.; Bloch, E. D.; Herm, Z. R.; Bae, T. H.; Long, J. R. *Chem. Rev.* **2012**, *112*, 724.
(22) Horcajada, P.; Gref, R.; Baati, T.; Allan, P. K.; Maurin, G.; Couvreur, P.; Ferey, G.; Morris, R. E.; Serre, C. *Chem. Rev.* **2012**, *112*, 1232.
(23) Wang, Z.; Cohen, S. M. *Chem. Soc. Rev.* **2009**, *38*, 1315.
(24) Eddaoudi, M.; Kim, J.; Rosi, N.; Vodak, D.; Wachter, J.; O'Keeffe, M.; Yaghi, O. M. *Science* **2002**, *295*, 469.
(25) Ockwig, N. W.; Delgado-Friedrichs, O.; O'Keeffe, M.; Yaghi, O. M. *Acc. Chem. Res.* **2005**, *38*, 176.
(26) Toussaint, L.; Bertrand, L.; Hue, L.; Crichton, R. R.; Declercq, J. P. *J. Mol. Biol.* **2007**, *365*, 440.
(27) Huard, D. J.; Kane, K. M.; Tezcan, F. A. *Nat. Chem. Biol.* **2013**, *9*, 169.
(28) Li, H.; Eddaoudi, M.; O'Keeffe, M.; Yaghi, O. M. *Nature* **1999**, *402*, 276.
(29) Barthelet, K.; Marrot, J.; Riou, D.; Ferey, G. *Angew. Chem., Int. Ed.* **2002**, *41*, 281.
(30) Santambrogio, P.; Pinto, P.; Levi, S.; Cozzi, A.; Rovida, E.; Albertini, A.; Artymiuk, P.; Harrison, P. M.; Arosio, P. *Biochem. J.* **1997**, *322*, 461.
(31) Lawson, D. M.; Artymiuk, P. J.; Yewdall, S. J.; Smith, J. M.; Livingstone, J. C.; Treffry, A.; Luzzago, A.; Levi, S.; Arosio, P.; Cesareni, G.; Thomas, C. D.; Shaw, W. V.; Harrison, P. M. *Nature* **1991**, *349*, 541.
(32) Liu, L.; Konstas, K.; Hill, M. R.; Telfer, S. G. J. *J. Am. Chem. Soc.* **2013**, *135*, 17731.
(33) Grams, F.; Reinemer, P.; Powers, J. C.; Kleine, T.; Pieper, M.; Tschesche, H.; Huber, R.; Bode, W. *Eur. J. Biochem.* **1995**, *228*, 830.
(34) Puerta, D. T.; Cohen, S. M. *Inorg. Chem.* **2002**, *41*, 5075.
(35) Schulze Wischeler, J.; Innocenti, A.; Vullo, D.; Agrawal, A.; Cohen, S. M.; Heine, A.; Supuran, C. T.; Klebe, G. *ChemMedChem* **2010**, *5*, 1609.
(36) Jani, M.; Tordai, H.; Trexler, M.; Banyai, L.; Patthy, L. *Biochimie* **2005**, *87*, 385.
(37) Radford, R. J.; Tezcan, F. A. J. *J. Am. Chem. Soc.* **2009**, *131*, 9136.
(38) Radford, R. J.; Nguyen, P. C.; Ditri, T. B.; Figueroa, J. S.; Tezcan, F. A. *Inorg. Chem.* **2010**, *49*, 4362.
(39) Radford, R. J.; Nguyen, P. C.; Tezcan, F. A. *Inorg. Chem.* **2010**, *49*, 7106.
(40) Radford, R. J.; Lawrenz, M.; Nguyen, P. C.; McCammon, J. A.; Tezcan, F. A. *Chem. Commun.* **2011**, *47*, 313.
(41) Burazerovic, S.; Gradinaru, J.; Pierron, J.; Ward, T. R. *Angew. Chem.* **2007**, *119*, 5606.
(42) Broomell, C. C.; Birkedal, H.; Oliveira, C. L. P.; Pedersen, J. S.; Gertenbach, J.-A.; Young, M.; Douglas, T. *Soft Matter* **2010**, *6*, 3167.
(43) Jung, S.; Kim, Y.; Kim, S.-J.; Kwon, T.-H.; Huh, S.; Park, S. *Chem. Commun.* **2011**, *47*, 2904.

DOI: 10.1021/jacs.5b07463
J. Am. Chem. Soc. 2015, 137, 11598−11601